



Study of equilibrium, Kinetic, thermodynamic and mechanism of trivalent chromium retention from tannery effluent by calcined layered double hydroxide

R. Lahkale*, R. Sadik*, W. ElHatimi, E. Khiar, E. Sabbar*

Laboratory of Physic and Chemistry of Materials (LPCM). Department of Chemistry, University Chouaïb Doukkali, El Jadida, MOROCCO.

Received 01 Feb 2016, Revised 11 Mar 2016, Accepted 25 Mar 2016

*Corresponding. E-mail: r.lahkale@hotmail.com; sadik084@yahoo.fr and esabbar@yahoo.fr; Tel. : +212667659110

Abstract

The removal of trivalent chromium from tannery effluent was carried out by adsorption using a mixed oxide of magnesium and aluminum obtained after calcination of a layered double hydroxide. This work requires the control and optimization of various parameters such as the effect of contact time, pH, adsorbent dose, chromium initial concentration and temperature. The removal of trivalent chromium from tannery effluent is a rapid process. In fact, in the ambient temperature (25°C), the adsorption equilibrium is reached after 30 min and the kinetic process is successfully fitted by pseudo-second-order model. In addition, the adsorption of trivalent chromium follows the Freundlich isotherm. The effect of temperature on the adsorption process of chromium was also studied and the thermodynamic parameters were determined.

Keywords: Layered double hydroxides; trivalent chromium; chromium adsorption; tannery effluent; thermodynamic parameters

1. Introduction

In nature, the presence of the chromium is in oxidation states between 2 and 6. However; only chromium (III) and (VI) are stable. This metal is widely used in various industrial applications such as metal finishing, tanning of skin, lining of wood and it's used in the chemistry of dyes, textile, magnetic tapes, as an anti-corrosion agent and water-cooling control... [1].

The tannery is the most important source of chromium contamination of the water in the world. The tanning with the chromium is highly demanded by the leather industry. Approximately 90% of this process uses the salts of trivalent chromium sulfate [2].

Unfortunately, this operation leaves a significant accumulation of this metal in the industrial discharge. At a high level, this accumulation can cause serious problems for humans and animals such as fish living in contaminated water. It can also cause skin diseases, tumors, infertility and respiratory problems [3].

However, Alkan et al. [4] have shown that at a concentration greater than 500 mg/L, chromium (III) has some toxicity affecting the digestion. The adsorption process is the most efficient technique that is widely used to eliminate this toxic heavy metal from the industrial water washing [5].

As the adsorption process using activated carbon is very expensive, it's a very interesting to find other cheaper substituents such as layered double hydroxides (LDH), which could be a good substituent in the removal of the contaminant from the industrial effluent [6-10]. The layered double hydroxides (LDH) or hydrotalcite-like compounds can be described by the general formula $[M^{2+}_{1-x}M^{3+}_x(OH)_2]^{x+}[X^{m-}_{x/m}, nH_2O]$ where M^{2+} is a cation of divalent metal, M^{3+} is cation of trivalent metal, X^{m-} represents an anion intercalated [11-13]. The calcination of these LDH gives mixed oxides which are non-stoichiometric intermediate [14] and by rehydration gives their counterparts with different intercalated anions, it is called memory effect. In this work, the adsorption of chromium from tannery effluent was performed by calcined hydrotalcite.

Various parameters were analyzed such as the effect of contact time, pH, adsorbent dose, initial chromium concentration and temperature.

2. Experiment

2.1. Analysis and characterization

All chemical reagents were of grade quality obtained from commercial sources and used without further purification.

Chemical composition of tannery effluent and metal were determined by ICP Emission Spectrophotometer.

IR spectra were recorded in the range of 4000–400 cm⁻¹ on a FT-IR-8400S SHIMADZU spectrometer using KBr pellets (2%).

The clay was characterized by X-ray diffraction using 2 -D-diffractometer of Bruker-AXS PHASER using copper K_{α1} radiation (1.54056 Å) and K_{α2} (1.54439 Å).

The dosage of chromium was carried out by spectrophotometry using a spectrophotometer type RAYLEIGH-Vis Spectrophotometer 7220G.

2.2. Synthesis of the adsorbent

The preparation of the precursor was carried out by the method of coprecipitation described by Reichle [11].

(MgCl₂, 6H₂O) and (AlCl₃, 6H₂O) are dissolved in distilled water with a molar ratio (Mg/Al = 3). The pH of the reaction mixture was maintained constant at 10.0 by addition of a mixture of NaOH and Na₂CO₃ ([NaOH]/[Na₂CO₃] = 4). The gel was stirred at room temperature for 48h. The clay obtained was washed by centrifugation with distilled water and dried at 60°C for 48 h. The chemical formula of the clay prepared is Mg_{2.95}Al(OH)_{7.9}(CO₃)_{0.5}·3.1H₂O (noted HT). The adsorbent used in this study is obtained by calcination of HT at 500°C during 5 h. The formula of this mixed oxide is Mg_{2.95}AlO_{4.45} (noted MgAlO).

2.3. Effluent sample

The effluent sample has been collected without further treatment from the modern tannery industry located in the greater Casablanca-Mohammedia (city in Morocco). This company uses the chromium (III) salt as basic chromium sulfate. The Cr(III) initial concentration is 4802 mg/L and the sulfate initial concentration is 29563 mg/L (Table 1).

Table 1 : Parameters effluent sample

Elements	C (mg/L)	Elements	C (mg/L)	Elements	C (mg/L)
Cr	4802	Zn	1,84	Mn	0,08
Na	19569	Ni	0,12	SO₄²⁻	29563
Ca	469	Mo	0,6	Cl ⁻	16040
Mg	111,7	Al	0,36		
Cd	0,07	Fe	6,9		

2.4. Batch Adsorption Studies

These experiments were performed by contacting 20 mg of MgAlO with 50 ml of tannery effluent at desired contact time, pH, adsorbent dose, initial Cr(III) concentration and temperature.

Once the equilibrium time was reached, the adsorbent was recovered by centrifugation.

The amount of Cr(III) retained per unit mass of solid at equilibrium is calculated by:

$$q_e = (C_0 - C_e)V/m \quad (1)$$

Where q_e (mg/g) is the amount of Cr(III) adsorbed per gramme of adsorbent; m (g) is the mass of the adsorbent, C_0 and C_e (mg/L) are the Cr(III) concentrations respectively at $t = 0$ and at equilibrium.

The Cr(III) removal efficiency or Cr(III) uptake (%) is calculated by:

$$(\%) = 100 (C_0 - C_e)/C_0 \quad (2)$$

The equilibrium chromium concentration was measured after two stages:

1-Oxidation at high temperature of Cr(III) present in effluent to Cr(VI) with KMnO_4 solution (5%), the excess of KMnO_4 was reduced by Na_3N solution (1%).

2-The residual Cr(VI) concentration in the solution was determined spectrophotometrically at 540 nm following the 1,5-diphenylcarbazide method [15].

3. Results and discussion

3.1.Characterization

3.1.1. X-ray diffraction

The typical XRD pattern (Fig. 1) shows a lamellar structure of LDH material. The XRD patterns are indexed in the R-3m space group, where c is the lattice parameter corresponding to three times the interlayer distances ($c=3d_{003}$).The peak (110) indicates the intermetallic distance used to calculate a (lattice parameter ($a=2d_{110}$)).

The values of the parameters c and a are respectively 23.13 and 3.02Å. These values are similar to those reported in literature [16, 17].

The characterization of the MgAlO performed by X-ray diffraction (Fig. 2) shows the production of mixed oxide. Indeed, the disappearance of the characteristic pic of the HT is observed. That is to say, the structure is destroyed due to dehydroxylation of the sheet with the departure of water molecules and anions CO_3^{2-} . Obtaining the mixed oxide is confirmed by the non presence of a characteristic peak of simple oxides [8].

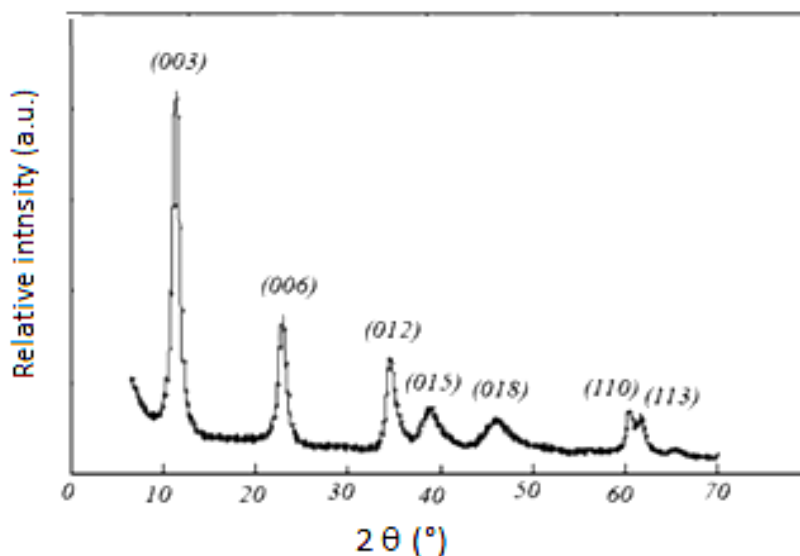


Figure 1: X-ray powder diffraction pattern of HT.

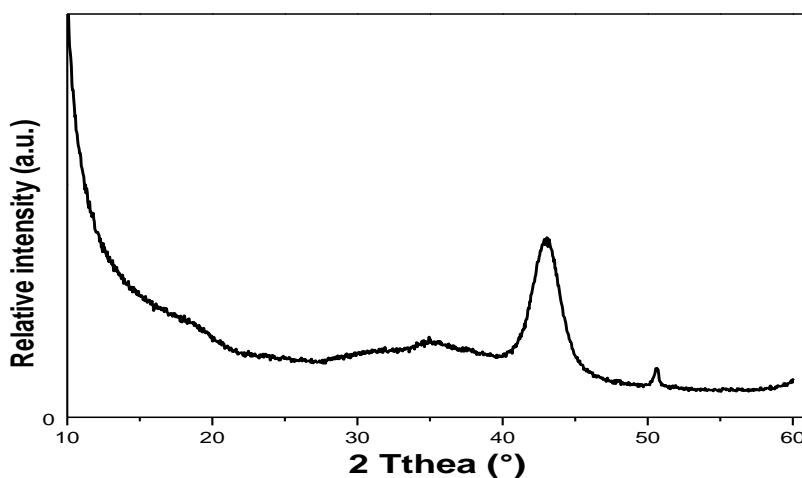


Figure 2: X-ray powder diffraction pattern of MgAlO.

3. 1. 2. Infrared Spectroscopy

From figure 3, we can observe:

A broad strong band at 3463 cm^{-1} which could be attributed to the stretching vibration of hydroxyl group. The low intensity band at 1637 cm^{-1} is assigned to bending vibration of strongly adsorbed water (solvation water for compensating anion vibration).

The band at 1381 cm^{-1} is assigned to carbonate vibration (CO_3^{2-}), the bands at 672 and 436 cm^{-1} are respectively due to M–O and O–M–O related to LDH layer (M is a divalent or trivalent metal) (Fig.3). These results are similar to those reported by Lv et al [16].

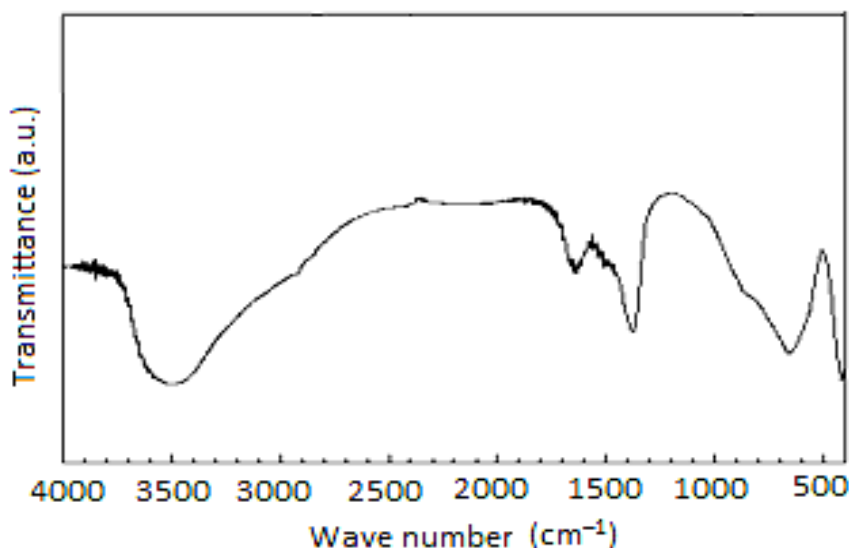


Figure 3: FTIR spectra for HT

3.2. Batch Adsorption Studies

3.2.1. Effect of contact time

The effect of contact time was studied from 5 to 90 min, the initial Cr (III) concentration in effluent was fixed to 48 mg/L.

Figure 4 shows that the adsorption equilibrium of Cr(III) by MgAlO is reached quickly after 30 min with 90,25% of Cr(III) uptake corresponding to 108,31 mg/g as adsorption capacity.

Such a rapid uptake is an indication a high affinity of Cr (III) for the active sites of the MgAlO [9, 18, 19].

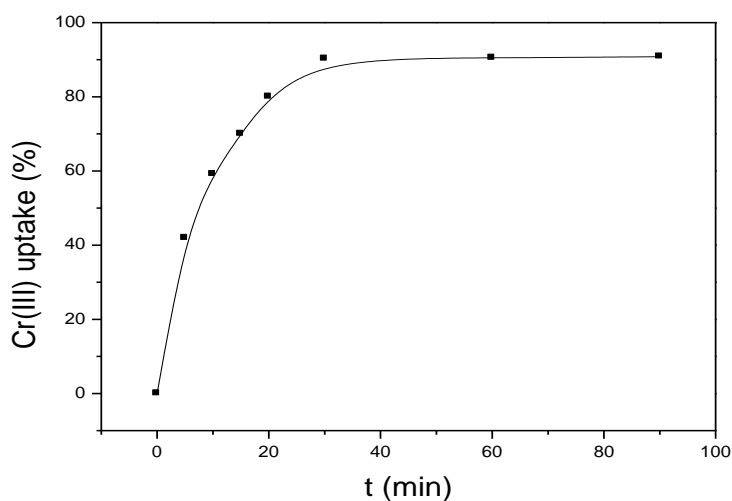


Figure 4: Effect of contact time (initial Cr (III) concentration: 48mg/L, adsorbent dose: 0,4 g/L, T: 25°C, pH4).

The adsorption kinetic was analyzed by the pseudo first-order equation [20], eq. (3) or pseudo-second order [21], eq. (4).

$$\ln(q_e - q_t) = \ln(q_e) - t.K_{1,ads} \quad (3)$$

$$t/q_t = t/q_e + 1/(q_e^2 \cdot K_{2,ads}) \quad (4)$$

q_e and q_t are the amounts of Cr(III) adsorbed by MgAlO respectively at equilibrium and t , $K_{1,ads}$ and $K_{2,ads}$, the adsorption constants. The experimental equilibrium data can be fitted by eq. (3) and (4), the value of R^2 (Fig.5 and 6) indicates that Cr (III) adsorption is successfully fitted by pseudo-second-order model.

The low value of the adsorption rate constant $K_{2,ads} = 0,00206 \text{ g.mg}^{-1}.\text{min}^{-1}$ confirms the rapid process identified by the kinetic study [9]. This behavior has been observed in the adsorption of Cr (III) by lignin [22].

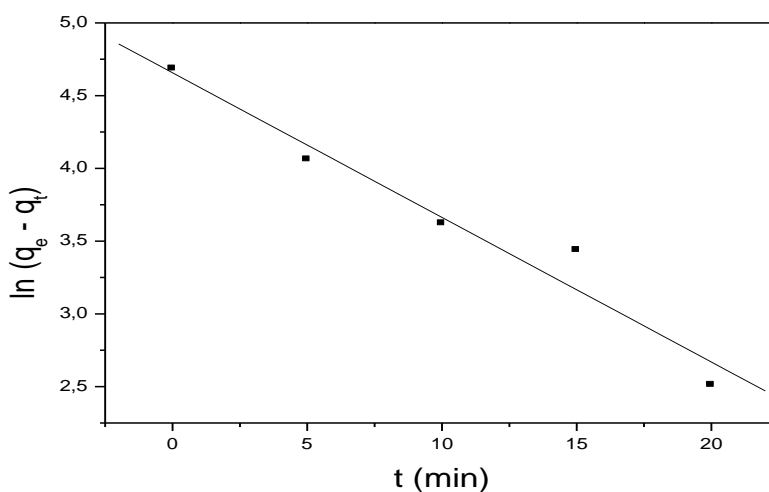


Figure 5: Model of first-order for Cr(III) adsorption by MgAlO.

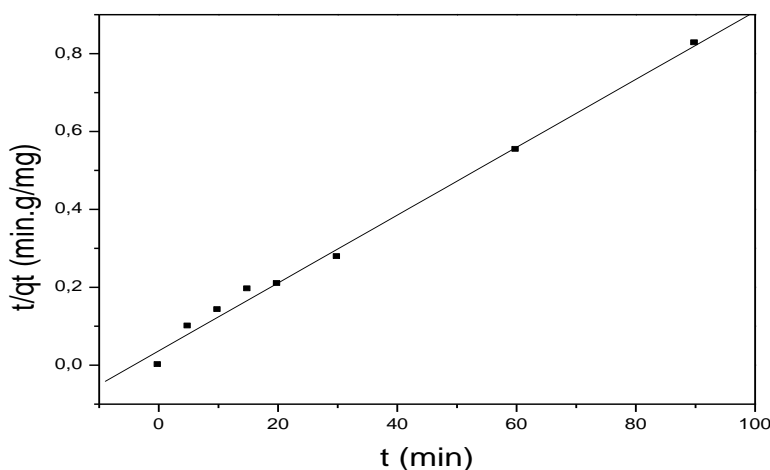


Figure 6: Model of pseudo-second-order for Cr(III) adsorption by MgAlO.

Table 2: Fitting parameters for the Cr(III) adsorption kinetic models

Model of pseudo first-order		Model of pseudo second-order	
$K_{1,ads}$	0,09941 min^{-1}	$K_{2,ads}$	0,00206 $\text{g.mg}^{-1}.\text{min}^{-1}$
q_e	105,32 mg/g	q_e	114,81 mg/g
R^2	0,97	R^2	0,99

The amount at equilibrium calculated by the pseudo second order model is $q_e = 114,81$ mg/g. These results are similar to those reported by adsorption kinetics ($q_e = 108,31$ mg/g).

3.2.2. Intradiffusion

The intra-particle diffusion approach [23] can be used to predict if intra-particle diffusion is the rate-limiting step. The experiment data exhibit multi-linear plots, revealing that the process is governed by two steps (Fig. 7). The first linear portion (phase I) at both concentrations can be attributed to the immediate utilization of the available sites on the sorbent surface. In contrast the phase II may be attributed to very slow diffusion of the sorbate Cr (III) from the surface site into the inner pores.

Thus the initial portion of Cr(III) sorption by MgAlO may be governed by the initial intra-particle transport of Cr^{3+} controlled by surface diffusion process and the later part controlled by pore diffusion. [10]

The values of ($k_{ip1} = 20,92$) and ($k_{ip2} = 0,16$) (diffusion rate constants for phases I and II, respectively) obtained from the slope of linear plots [23].

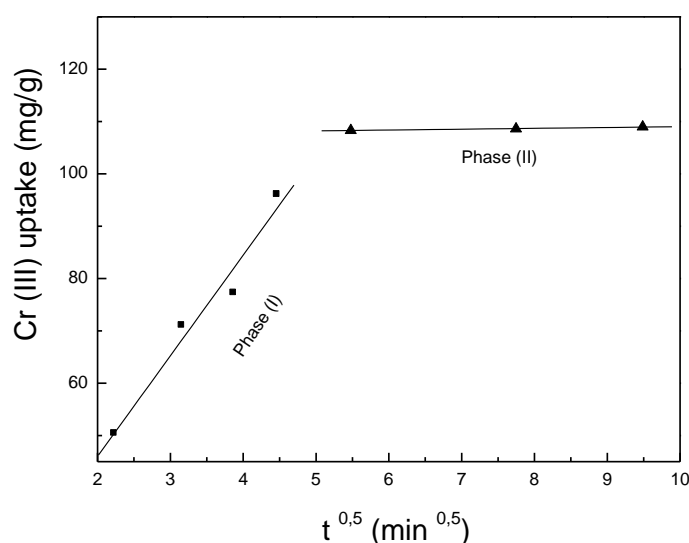
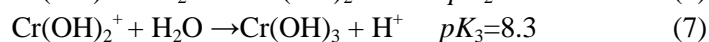
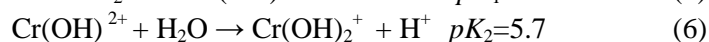
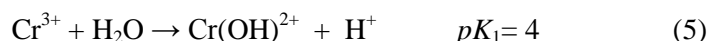


Figure 7: Intra-particle diffusion plots of sorption of chromium (III) on MgAlO

3.2.3 Effect of pH

The adsorption of metals depends strongly on the pH which is related to the surface charge of the adsorbent, to the degree of ionization or speciation of the metals.

Various types of mechanisms for the adsorption of metals by anionic or cationic clays are reported in literature such as ion exchange [24], electrostatic effect, interaction, complexation, chelation, precipitation [25], and isomorphous substitution [26]. These mechanisms were determined from the surface properties of the adsorbent, its resistance to the pH and the nature of the intercalated ions. The behavior of metal ions in the effluent solution is complex because these ions are presented with different degrees of activity and opposite charge. So, it's necessary to clarify the nature of different hydrolyzed species of the chromium at various pH values. The percentages of hydrolyzed species of chromium are calculated from their equilibrium constant of hydrolysis [27]:



As to our study, the pH effect is studied between 2 and 8.3 for an effluent chromium concentration of 48 mg / L and a dose of 0,4 g/L MgAlO (Fig. 9). The maximum retention is obtained at pH = 4. According to the pH diagram (Fig. 8), we can conclude that the chromium is retained in cationic form. This will be confirmed at the end of this work.

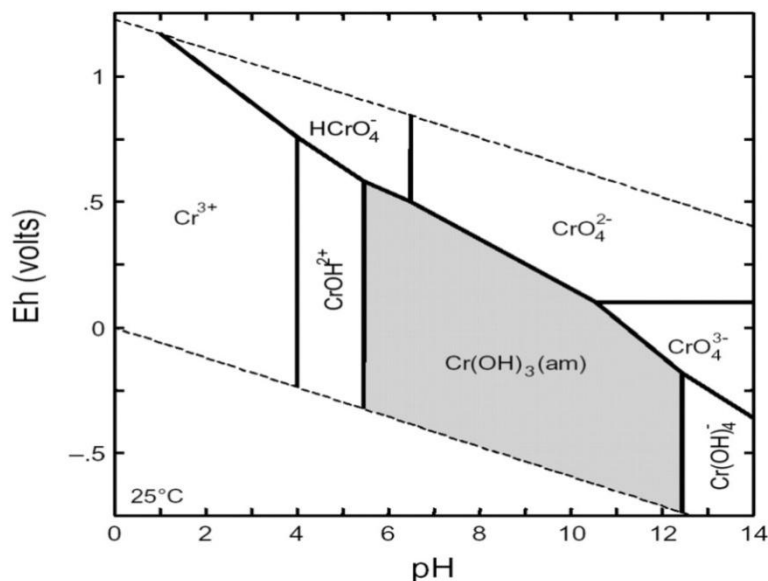


Figure 8: Speciation diagram of chromium (III).

Beyond this value, we note a decrease in the retention percentage which can be explained by the existence of other competitive species in the effluent (Table 1). The retention observed between 6 and 8,3 can't be attributed to our adsorbent but to a precipitation reaction of Cr(OH)₃ [28].

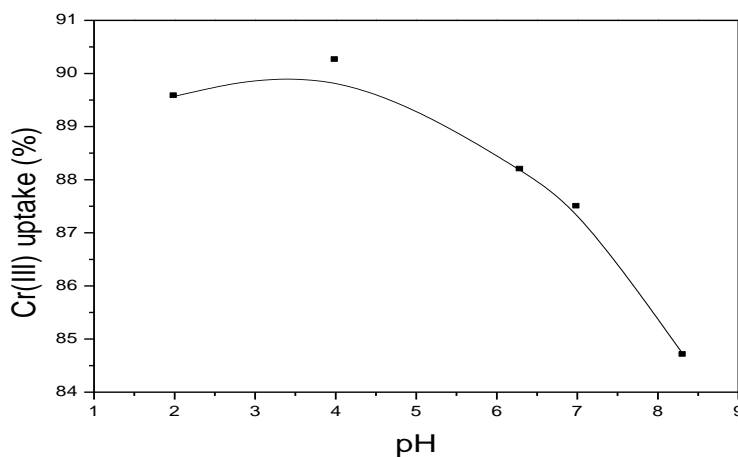


Figure 9: Effect of initial pH (MgAlO dose : 0,4 g/L, initial [Cr(III)] :48 mg/L, t : 30 min, T : 25°C)

3. 2. 4. Effect of adsorbent dose

The effect of adsorbent dose was studied by varying the amount of the adsorbent from 0,1 to 1,2 g /L, initial concentration of chromium effluent was fixed at 48 mg/L.(Fig.10)

This study shows that the removal efficiency of Cr (III) increases from 23,92 to 90,25% when the dose of MgAlO increases of 0,1 g / L at a value of 0,4 g /L and stabilizes thereafter. This can be explained by the fact that at low dose MgAlO, the number of adsorption sites available to accommodate the high number of Cr (III) effluent is insufficient which causes low efficiency of elimination. However, at high doses of MgAlO, the number of adsorption sites is sufficient to retain the maximum ion Cr (III).

Any increase of the dose of MgAlO no net effect on the efficiency of Cr (III). Explained usually by poor dispersion of the adsorbent in solution, due to agglomeration of the clay, this phenomenon usually causes a decrease in retention [9].

However, at high doses of MgAlO, the number of adsorption sites is sufficient to retain the maximum ion Cr (III). Similar results were reported for the adsorption of Cr(III) from a tannery by a cationic clay [29]. Furthermore, the dose of MgAlO which is considered sufficient for maximum elimination of Cr (III) effluent is 0,4g/ L.

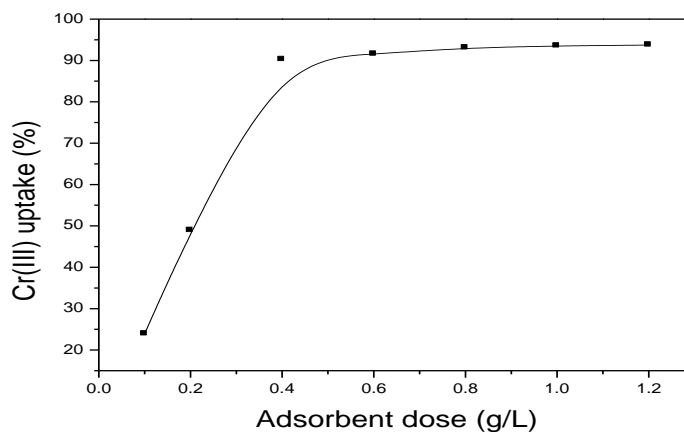


Figure 10: Effect of MgAlO dose (initial Cr(III) concentration: 48 mg/L, pH4, T: 25°C.

3. 2. 5. Effect of initial chromium concentration

The effect of initial concentration of Cr(III) was studied by varying the Cr(III) concentration in effluent from 4.8 mg/L to 120 mg/L at 298 K, adsorbent dose was taken to 0,4 g/L.

Figure 11 shows that if the concentration of Cr (III) increases, the MgAlO adsorption capacity increases, which suggests that the valuation of optimal ratio adsorbate / adsorbent is beyond 120 mg concentration of Cr (III).

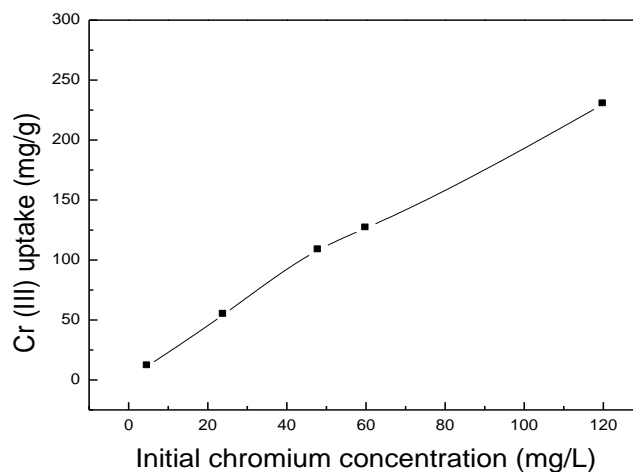


Figure 11: Effect of initial Cr (III) concentration ($t_{eq} = 30$ min, MgAlO dose: 0,4 g/L, T: 25°C, pH 4)

3. 2. 6. Adsorption isotherm

The experimental equilibrium data can be interpreted by Langmuir and Freundlich equations (8) and (9):

$$C_e/q_e = 1/(K_L \cdot q_m) + (1/q_m)C_e \quad (8)$$

$$\ln q_e = \ln (K_F) + (1/n)\ln C_e \quad (9)$$

Where q_e is the amount of Cr(III) adsorbed by MgAlO at equilibrium; q_m is the saturated adsorption capacity of the Cr(III) by MgAlO; K_L , a constant of the Langmuir isotherm and C_e , the equilibrium concentration of the Cr(III) in effluent; K_F and $1/n$ are the parameters of the Freundlich isotherm.

The experimental equilibrium data can be fitted by the equations (8) and (9), the value of R^2 (0,99 for Freundlich and 0,96 for Langmuir isotherm) indicates that Cr(III) adsorption is successfully fitted by the Freundlich isotherm model (Fig.12 and 13).

The maximum capacity K_F is 36,57 mg/g (L/mg)^{1/n}, and the adsorption constant 1/n is 0,57. The value of 1/n between 0 and 1 represent good adsorption of Cr (III) on MgAlO [9, 30].

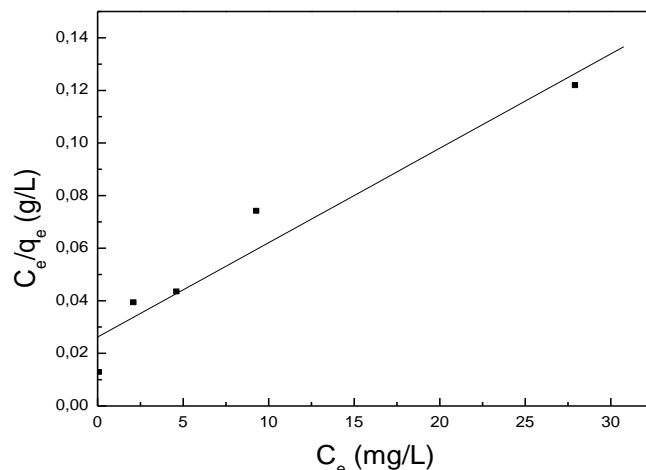


Figure 12: Langmuir isotherm for Cr (III) adsorption by MgAlO.

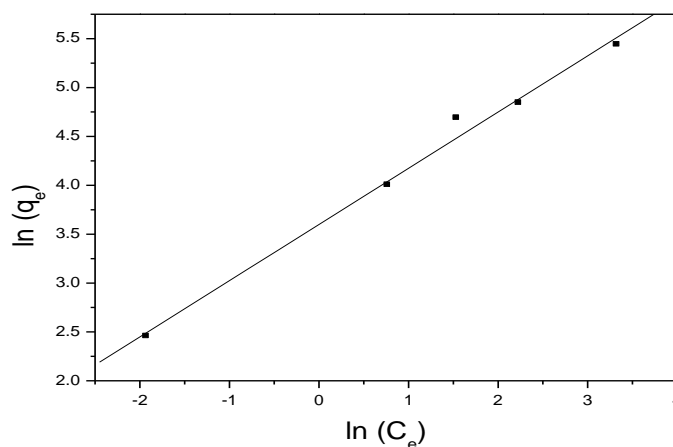


Figure 13: Freundlich isotherm for Cr(III) adsorption by MgAlO.

3.2.7. Effect of temperature

The effect of temperature was studied for four temperatures 298, 308, 318 and 328 K in a time interval from 10 to 90 minutes. The Cr (III) concentration in effluent was taken to 120 mg/L. The effect of temperature (Fig. 14) on the adsorption process was determined using equations:

$$K_c = q_e/C_e \quad [31] \quad (10)$$

$$\ln K_c = \Delta S^\circ/R - \Delta H^\circ/RT \quad (11)$$

$$\Delta G^\circ = -RT \ln K_c \quad (12)$$

Where : K_c is the equilibrium constant, q_e is the adsorption capacity (mg g⁻¹) of the adsorbent for Cr(III) after time (t) of adsorption and is obtained from the slope of the plot of t/q_t versus t (Fig. 15) using Eq. (4) and (10), C_e is equilibrium concentration (mg/L) of Cr(III) after time t of adsorption onto adsorbent. ΔG° is the change in Gibbs free energy,

ΔS^0 is the change in entropy,
 ΔH^0 is the change in enthalpy,
 R is the gas constant ($= 8.314 \text{ J.mol}^{-1} \text{ K}^{-1}$),
 T is the adsorption temperature (K).

The values of ΔS^0 and ΔH^0 were determined by plotting $\ln K_c$ versus $1/T$ (Fig. 16) and using Eq. (11). The value of ΔG^0 was calculated from Eq. (12). The positive value of ΔH^0 indicates that adsorption is endothermic. The negative value of ΔG^0 confirms the spontaneous nature of the adsorption. The increase of ΔG^0 with temperature indicates that the adsorption process is favorable at high temperature. According to Alkan et al. [32], the adsorption is chemisorption when the value in ΔH^0 is between 40 and 120 kJ.mol^{-1} . The result obtained in this study is $65.44 \text{ kJ.mol}^{-1}$ (Table3) indicates that the adsorption of Cr (III) by MgAlO is chemisorption. The positive value of ΔS^0 (Table3) suggests the increased randomness at the solid/solution interface for the removal of Cr (III) in effluent.

Similar results were found for the adsorption of Pb (II) by $\text{Mg}_2\text{Al-LDH}$ [33] or for the defluoridation of drinking water by calcined MgAl-CO_3 layered double hydroxides [34].

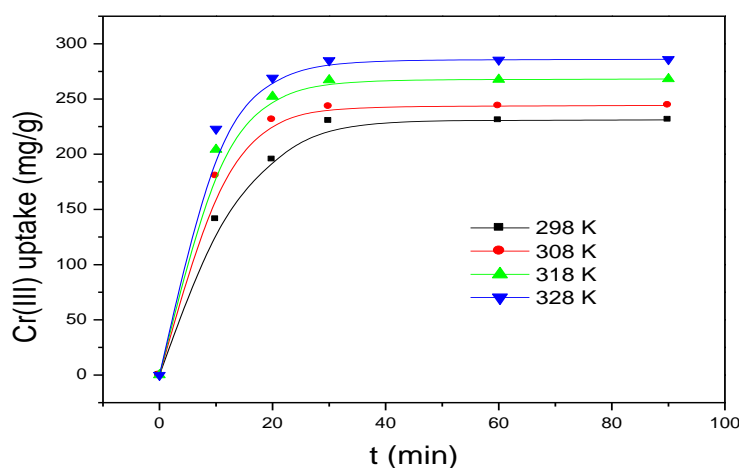


Figure 14: Kinetic plots of Cr (III) adsorption (initial [Cr(III)] in effluent: 120mg/L, MgAlO dose: 0,4g/L, pH4)

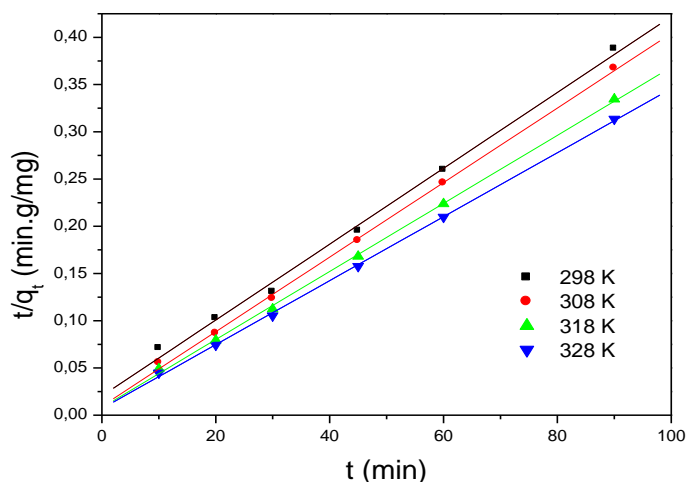


Figure 15: Pseudo-second order plots for Cr(III) adsorption by MgAlO (initial Cr(III) concentration in effluent: 120mg /L, MgAlO dose: 0,4 g/L, pH4)

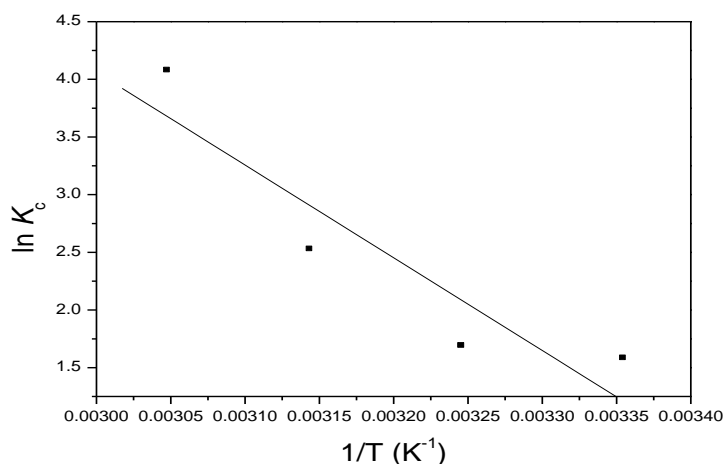


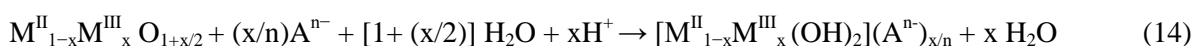
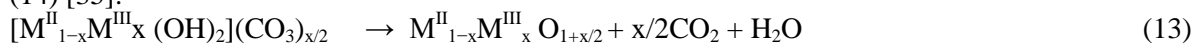
Figure 16 : Van't Hoff plot for Cr (III) adsorption by MgAlO.

Table 3: Thermodynamic parameters for adsorption of Cr(III) in effluent by MgAlO

T (K)	ΔG° (kJ mol ⁻¹)	ΔH° (kJ mol ⁻¹)	ΔS° (J mol ⁻¹ K ⁻¹)
298	-2,90	65,44	229,36
308	-5,20		
318	-7,40		
328	-9,79		

3.2.8. Retention mechanism

Calcination of these HT produces intermediate non-stoichiometric oxides [14], which undergo rehydration and incorporation of anions in aqueous medium to regain the hydroxalite structure as expressed by Eqs. (13) and (14) [35]:



In this study the retention mechanism makes a reconstruction of MgAl-SO₄ LDH followed of adsorption sulfate anions at the surface, because the sulfate anions has a height affinity for adsorbent [14], also sulfate has a height concentration in effluent (table1) (MgAl-SO₄ LDH) of which sulfate anions are bound chromium ions MgAl-SO₄/Cr. This result is confirmed by the characterization of the product recuperated after adsorption by XRD. In effect, the X diffractogram obtained (Fig. 17) shows the shape type of a LDH.

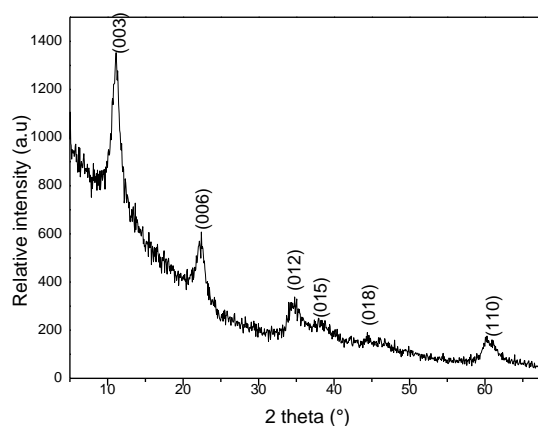


Figure 17: XRD pattern of MgAlO after adsorption

Thus, the interlamellar distance of the order of 7,93Å is less than that which is obtained in the usually synthesis of MgAl-SO₄ phase. This can be explained by the preferential orientation of sulfate anion when regenerating HT-SO₄ by the reconstruction method. [36]

In addition, the characteristic bands of LDH, the study by infrared spectroscopy of the product obtained (Fig. 18) confirms the presence of sulfate ions by the appearance of three characteristic bands at 620, 1110 and 1190 cm⁻¹.

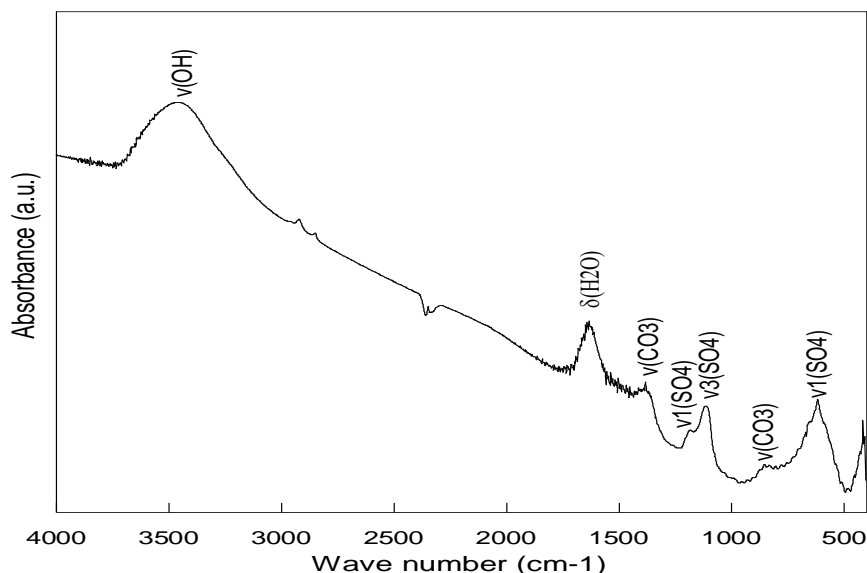


Figure 18: FTIR spectra for MgAlO after adsorption.

From the above results we can proposed the following mechanism (Fig.19):

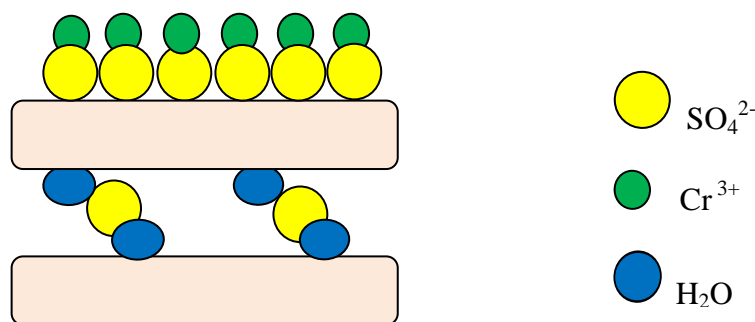


Figure 19: Model of the retention mechanism

Conclusions

From the above results of the adsorption of Cr(III) effluent by MgAlO obtained after calcination of Mg₃Al-CO₃ LDH at 500 °C during 5h under these experimental conditions, the following conclusions can be made:

- The adsorption equilibrium is quick and the kinetic process is successfully fitted by pseudo-second-order model.
- Cr (III) removal efficiency increases when the pH increases from 2 to 4, and decreases gradually at pH ≥ 4 (pH 4 is the optimal value).
- Cr (III) removal efficiency increases with the increase of MgAlO dose from 0,1g/L to a maximum value (0,4 g/L, optimal value).
- The adsorption process follows the Freundlich isotherm model and the saturated adsorption capacity of MgAlO is 36,57 (mg/g)(L/mg)^{1/n}.
- The adsorption is chimisorption process, spontaneous and endothermic in nature.
- The retention mechanism makes a reconstruction of MgAl-SO₄ LDH, which is confirmed by XRD result.

The above results permit to conclude that calcined hydroxalcalite exhibit an interesting adsorption properties removing the trivalent chromium from tannery effluent.

Acknowledgements The authors would like to thank the research group in the Laboratory of Physic and Chemistry of Materials (LPCM) at the Faculty of Sciences in El Jadida, for their great support for the realization of this work.

References

1. Shah B. A., Shah A.V., Singh R.R., *Inter. J. Enviro.Sci and Tech.* 6(1) (2009) 77-90.
2. Sundar V.J., Rao J.R., Muralidharan C., *J. Clean. Prod.* 10 (2002) 69-74.
3. Natale F. Di., Lancia A., Molino A., Musmarra D., *J. Hazard Mater.* 145 (2007) 381-390.
4. Alkan U., Anderson G.K., Ince O., *Wat. Res.* 30(3) (1996) 731-741.
5. Ghiassi K., Smith E., *J. Water Environ, Res.* (2006) 84- 93.
6. Lazaridis N.K., Asouhidou D.D., *Water Res.* 37(12) (2003) 2875-82.
7. Sadik N., Mountadar M., Sabbar E., *J. Mater. Environ. Sci.* 6 (8) (2014) 2239-2246.
8. Sadik R., Lahkale R., Hssaine N., ElHatimi W., Diouri M., Sabbar E., *J. Mater. Environ. Sci.* 6 (10) (2015) 2895-2905.
9. Lahkale R., Sadik R., Sabbar E., *J. Mater. Environ. Sci.* 5 (S2) (2014) 2403-2408.
10. Sadik R., Lahkale R., Hssaine N., Diouri M., Sabbar E., *IOSR-JESTFT* 8 (8) (2014) 28-36.
11. Reichle WT., *Solid State Ionics.* 22 (1986) 135-141.
12. Sabbar E., Marie E. R., Fabrice L., *Microporous Mesoporous Mater.* 103 (2007) 134-141.
13. Sabbar E., Marie E. R., Fabrice L. *J. Phys. Chem. Solids.* 67 (2006) 2419-2429.
14. Miyata S., *Clays Clay Miner.* 28(1) (1980) 50-56.
15. APHA, AWWA, WEF. 20th ed. American Public Health Association, American Water Work Association and Water Environment Federation, (1998) Washington, DC, USA.
16. Lv L., He J., Wei M., Evans DG., Duan X., *Water Research.* 40(4) (2006) 735-743.
17. Li Y., Gao B., Wu T., Wang B., Li X., *J. Hazard. Mater.* 164 (2009) 1098-1104.
18. Espantaleon A.G., Nieto J.A., Fernandez M., Marsal A., *Clays Clay Miner.* 24 (2003) 105-110.
19. Setshedi K., Ren J., Aoyi O., Onyango MS. *Int. J. Phys. Sci.* 7(1) (2011) 63-72.
20. Lagergren S., *Handl.Bihay.* 24 (Afd 1) (1898) 39.
21. Ho Y.S., McKay G., *Water Res.* 34 (2000) 735-742.
22. Wu Y., Zhang S., Guo X., Huang H., *Bioresour. Technol.* 99 (2008) 7709-7715.
23. Weber W. J., Morris J.C., *J. Sanit. Eng. Div. ASCE.* 89 (1963) 31-60.
24. Ibanez J.P., Umetsu Y., *Hydrometallurgy.* 72 (2004) 327-334.
25. Pavlovic I., Pérez M.R., Barriga C., Ulibarri MA., *Appl. Clay Sci.* 43 (2009) 125-129.
26. Pérez M.R., Pavlovic I., Barriga C., Cornejo J., Hermosín M.C., Ulibarri M.A., *Appl. Clay Sci.* 32 (2006) 245-251.
27. Kragten J., *Chichester/New York.* (1978) 223-234.
28. Lyva R., Ramos. L., Fuentes-Rubio R.M., Guerrero-coronado., Mendoza-Barron J., *J. Chem. Tech. Biotechnol.* 62 (1995) 64-67.
29. Tahir S.S., Naseem R., *Sep. Purif. Technol.* 53 (2007) 312-321.
30. Das J., Patra B.S., Baliarsingh B.S., Parida K.M., *Appl. Clay Sci.* 32 (2006) 252-260.
31. Unuabonah E.I., Adebowale K.O., Olu-Owolabi B.I. *J. Hazard. Mater.* 144 (2007) 386-395.
32. Zhao D., Sheng G., Hu J., Chen C., Wang X., *Chem. Eng. J.* 171 (2011) 167-174.
33. Alkan M., Demirbas O., Celikcapa S., Dogan M., *J. Hazard. Mater.* 116 (2004) 135-145.
34. L. Lv. *Desalination.* 208 (2007) 125-133.
35. Chatelet L., Bottero J.Y., Yvon J., Bouchelaghem.A., *Colloids Surf. A.* 111 (1996) 167-175.
36. Cardoso L. P., Valim. J. B., *J. Phys. Chem. Solids.* 67 (2006) 987- 993.

(2016) ; <http://www.jmaterenvirosnci.com/>